

## Report

## A Novel Role for Bcl-2 in Regulation of Cellular Calcium Extrusion

Pawel E. Ferdek,<sup>1</sup> Julia V. Gerasimenko,<sup>1</sup> Shuang Peng,<sup>1,2</sup> Alexei V. Tepikin,<sup>3</sup> Ole H. Petersen,<sup>1</sup> and Oleg V. Gerasimenko<sup>1,\*</sup>

<sup>1</sup>Medical Research Council Group, School of Biosciences, Cardiff University, Cardiff CF10 3AX, Wales, UK

<sup>2</sup>Department of Physiology, Medical College, Jinan University, Guangzhou 510632, China

<sup>3</sup>The Physiological Laboratory, Department of Cellular and Molecular Physiology, Institute of Translational Medicine, University of Liverpool, Liverpool L69 3BX, UK

## Summary

The antiapoptotic protein Bcl-2 [1, 2] plays important roles in  $\text{Ca}^{2+}$  signaling [3] by influencing inositol triphosphate receptors and regulating  $\text{Ca}^{2+}$ -induced  $\text{Ca}^{2+}$  release [4–6]. Here we investigated whether Bcl-2 affects  $\text{Ca}^{2+}$  extrusion in pancreatic acinar cells. We specifically blocked the  $\text{Ca}^{2+}$  pumps in the endoplasmic reticulum and assessed the rate at which the cells reduced an elevated cytosolic  $\text{Ca}^{2+}$  concentration after a period of enhanced  $\text{Ca}^{2+}$  entry. Because external  $\text{Ca}^{2+}$  was removed and endoplasmic reticulum  $\text{Ca}^{2+}$  pumps were blocked,  $\text{Ca}^{2+}$  extrusion was the only process responsible for recovery. Cells lacking Bcl-2 restored the basal cytosolic  $\text{Ca}^{2+}$  level much faster than control cells. The enhanced  $\text{Ca}^{2+}$  extrusion in cells from Bcl-2 knockout (Bcl-2 KO) mice was not due to increased  $\text{Na}^+/\text{Ca}^{2+}$  exchange activity, because removal of external  $\text{Na}^+$  did not influence the  $\text{Ca}^{2+}$  extrusion rate. Overexpression of Bcl-2 in the pancreatic acinar cell line AR42J decreased  $\text{Ca}^{2+}$  extrusion, whereas silencing Bcl-2 expression (siRNA) had the opposite effect. Loss of Bcl-2, while increasing  $\text{Ca}^{2+}$  extrusion, dramatically decreased necrosis and promoted apoptosis induced by oxidative stress, whereas specific inhibition of  $\text{Ca}^{2+}$  pumps in the plasma membrane (PMCA) with caloxin 3A1 reduced  $\text{Ca}^{2+}$  extrusion and increased necrosis. Bcl-2 regulates PMCA function in pancreatic acinar cells and thereby influences cell fate.

## Results and Discussion

Loss of Bcl-2 Affects  $\text{Ca}^{2+}$  Signaling in Pancreatic Acinar Cells

In this study, we compared  $\text{Ca}^{2+}$  signaling mechanisms, with a particular emphasis on  $\text{Ca}^{2+}$  extrusion, in pancreatic acinar cells isolated from Bcl-2 knockout (Bcl-2 KO) and control mice. We used a protocol allowing us to monitor the rate of reducing the cytosolic  $\text{Ca}^{2+}$  concentration ( $[\text{Ca}^{2+}]_i$ ) following a maximal elevation of  $[\text{Ca}^{2+}]_i$  during complete blockade of  $\text{Ca}^{2+}$  uptake into the endoplasmic reticulum (ER) (Figures 1A and 1B). Wild-type (WT) and Bcl-2 KO cells exposed to a  $\text{Ca}^{2+}$ -free solution were treated with thapsigargin (Tg), a specific inhibitor of  $\text{Ca}^{2+}$  pumps in the ER, in order to empty the ER  $\text{Ca}^{2+}$  stores. The extracellular  $\text{Ca}^{2+}$  concentration

( $[\text{Ca}^{2+}]_o$ ) was then increased to 1 mM, 5 mM, or 10 mM, which induced rapid influx of  $\text{Ca}^{2+}$  to the cytosol. After a stable  $[\text{Ca}^{2+}]_i$  plateau had been attained, extracellular  $\text{Ca}^{2+}$  was removed and  $[\text{Ca}^{2+}]_i$  declined until the baseline level had been reestablished (Figures 1A and 1B). Comparing the initial  $[\text{Ca}^{2+}]_i$  of WT and Bcl-2 KO cells, as shown in Figures 1A and 1B, we found that Bcl-2 KO cells had a significantly lower  $[\text{Ca}^{2+}]_i$  ( $57.5 \pm 3$  nM SE) than WT cells ( $100.3 \pm 5.6$  nM SE) (Figure 1C). This significant difference suggests important changes in equilibrium between  $\text{Ca}^{2+}$  entry and extrusion across the plasma membrane.

Loss of Bcl-2 Enhances  $\text{Ca}^{2+}$  Extrusion across the Plasma Membrane

Because  $\text{Ca}^{2+}$  uptake into the ER was blocked by Tg, the rate of decline of  $[\text{Ca}^{2+}]_i$ —after removal of external  $\text{Ca}^{2+}$ —must reflect the rate of  $\text{Ca}^{2+}$  extrusion. Calcium extrusion rates ( $d[\text{Ca}^{2+}]_i/dt$ ) were calculated and then plotted as a function of the  $[\text{Ca}^{2+}]_i$  values obtained from the exponential fit. Initial  $d[\text{Ca}^{2+}]_i/dt$  values (for the highest  $[\text{Ca}^{2+}]_i$ ) from each trace were plotted together on a graph and fitted by linear regression (Figure 1D). Similar results were obtained when we compared rates of recovery in cells treated with a high dose of Tg (10  $\mu\text{M}$ ) and acetylcholine (ACh) (see Figures S1A and S1B available online) or Tg alone (Figures S1C and S1D). The half-time of recovery of baseline  $[\text{Ca}^{2+}]_i$  levels in the experiments shown in Figures 1A and 1B was calculated, and the results demonstrate that recovery in Bcl-2 KO cells was much faster than in WT cells (Figure 1E).

 $\text{Ca}^{2+}$  Extrusion in Pancreatic Acinar Cells Is Mainly Dependent on Plasma Membrane Calcium-Activated ATPase

Tg blocks very specifically the ER  $\text{Ca}^{2+}$  pumps (sarcoendoplasmic reticulum  $\text{Ca}^{2+}$ -activated ATPase [SERCA]). In such conditions,  $\text{Ca}^{2+}$  removal from the cytosol is only dependent on  $\text{Ca}^{2+}$  export across the plasma membrane. The two main proteins responsible for this process are the plasma membrane calcium-activated ATPase (PMCA) [7] and the  $\text{Na}^+/\text{Ca}^{2+}$  exchanger (NCX) [8]. However, available evidence indicates that NCX plays a very minor, if any, role in  $\text{Ca}^{2+}$  extrusion from normal pancreatic acinar cells [9] and that therefore  $\text{Ca}^{2+}$  removal across the plasma membrane in these cells is mediated by PMCA.

 $\text{Na}^+/\text{Ca}^{2+}$  Exchange Does Not Contribute to  $\text{Ca}^{2+}$  Extrusion in WT and Bcl-2 KO Cells

In order to test independently, in pancreatic acinar cells, whether NCX plays any significant role in  $\text{Ca}^{2+}$  extrusion, we performed two different series of experiments. In the first, we replaced all  $\text{Na}^+$  in the external solution with N-methyl D-glucamine (NMDG<sup>+</sup>). This approach has been used frequently to inhibit NCX in the plasma membrane [10, 11]. We compared the  $\text{Ca}^{2+}$  extrusion rates, following removal of external  $\text{Ca}^{2+}$  in the presence of Tg, in WT (Figures S2A and S2B) and Bcl-2 KO cells (Figures S2C and S2D) and summarized the results by calculating the average half-time of recovery of the basal  $[\text{Ca}^{2+}]_i$  (Figure 1F). In experiments on

\*Correspondence: [gerasimenkoov@cardiff.ac.uk](mailto:gerasimenkoov@cardiff.ac.uk)

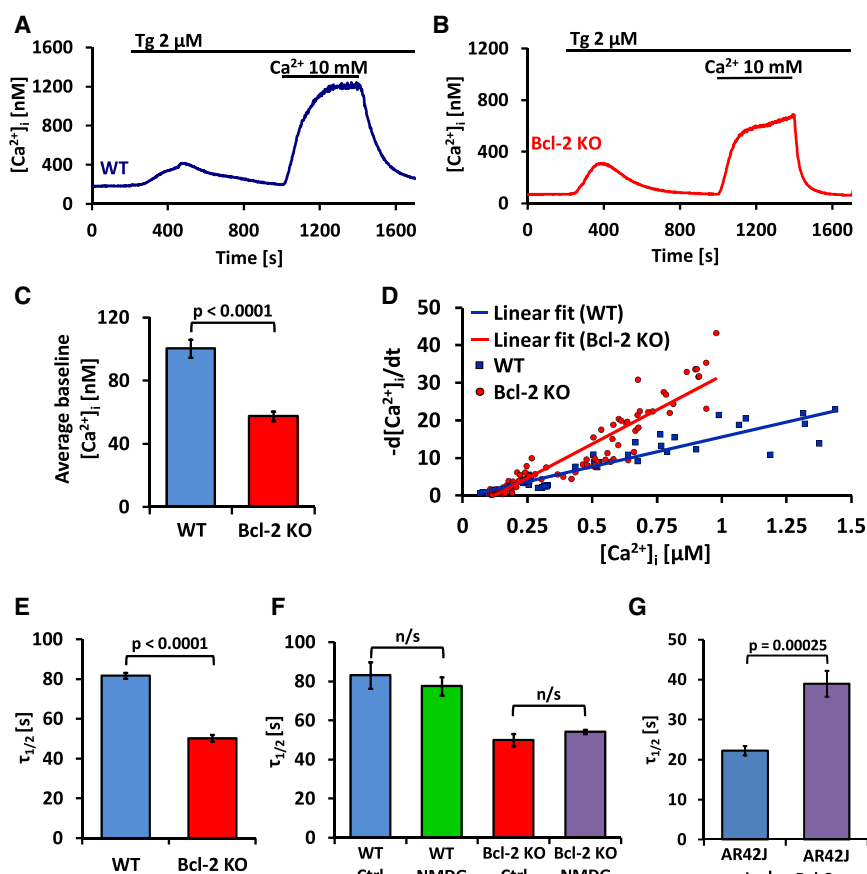


**Figure 1. Loss of Bcl-2 Protein Is Associated with Increased  $Na^+$ -Independent  $Ca^{2+}$  Extrusion across the Plasma Membrane**

(A) Typical  $[Ca^{2+}]_i$  trace recorded in a normal (WT) pancreatic acinar cell. Changes in  $[Ca^{2+}]_i$  were evoked first by application of thapsigargin (Tg) in the absence of external  $Ca^{2+}$  and thereafter by exposure, for a period of 400 s, to an external solution containing 10 mM  $Ca^{2+}$ . The reduction in the elevated  $[Ca^{2+}]_i$  following removal of the high  $Ca^{2+}$  external solution can, in the continued presence of Tg, only be due to  $Ca^{2+}$  extrusion across the plasma membrane.

(B) Pancreatic acinar cell from Bcl-2 KO mouse. The same protocol was used as in (A). The rate of reducing  $[Ca^{2+}]_i$  (due to  $Ca^{2+}$  extrusion) after removal of 10 mM external  $Ca^{2+}$  was much faster than in the WT cell (shown in A). The resting  $[Ca^{2+}]_i$  was also lower than in the WT cell.

(C) Comparison of the initial (resting, baseline)  $[Ca^{2+}]_i$  in WT (blue bar,  $n = 34$ ) and Bcl-2 KO (red bar,  $n = 109$ ) pancreatic acinar cells ( $p < 0.0001$ ). Data in (C) and (E)–(G) are presented as mean  $\pm$  SEM.

(D) Dependence of the initial rate of  $Ca^{2+}$  extrusion on  $[Ca^{2+}]_i$ , calculated from experiments of the type shown in (A) and (B), i.e., WT (blue,  $n = 34$ ) and Bcl-2 KO (red,  $n = 109$ ) pancreatic acinar cells. In cells from Bcl-2 KO mice,  $Ca^{2+}$  extrusion was much faster. See also Figure S1.

(E) Bar chart comparing half-times ( $\tau_{1/2}$ ) of the reduction in  $[Ca^{2+}]_i$  toward the resting level following removal of external  $Ca^{2+}$  in WT (blue bar,  $n = 20$ ) and Bcl-2 KO (red bar,  $n = 38$ ) cells.

(F) Bar chart comparing half-times ( $\tau_{1/2}$ ) of the reduction in  $[Ca^{2+}]_i$  toward the resting level following removal of external  $Ca^{2+}$  in WT pancreatic acinar cells in the normal presence of

external  $Na^+$  (blue bar,  $n = 18$ ) with those obtained when external  $Na^+$  was replaced by NMDG $^+$  (green bar,  $n = 24$ ) as well as in Bcl-2 KO cells (red bar,  $n = 25$ ). See also Figure S2.

(G) Bar chart comparing half-times ( $\tau_{1/2}$ ) of the reduction in  $[Ca^{2+}]_i$  toward the resting level following removal of external  $Ca^{2+}$  in control AR42J cells (blue bar,  $n = 14$ ) and in AR42J cells transfected with pcDNA3 Bcl-2 plasmid (Bcl-2 overexpression [oe]) (purple bar,  $n = 17$ ). Data were collected from cells expressing cytosolic Cameleon YC3.60. See also Figure S3.

both WT and Bcl-2 KO cells, removal of external  $Na^+$  had no effect on the rate of  $Ca^{2+}$  extrusion, as the half-times of the recovery of the basal  $[Ca^{2+}]_i$  were very similar to controls when  $Na^+$  was replaced by NMDG $^+$ .  $Ca^{2+}$  extrusion across the plasma membrane is therefore independent of the presence or absence of external  $Na^+$ , and the enhanced rate of  $Ca^{2+}$  extrusion observed in Bcl-2 KO cells cannot be explained by recruitment of NCX but must be due to increased  $Ca^{2+}$  outflux mediated by PMCA.

In the second series of experiments, we used  $LaCl_3$  as a blocker of PMCA. It has previously been shown that 1 mM lanthanum abolishes  $Ca^{2+}$  extrusion by PMCA without affecting NCX [12]. As seen in Figures S2E and S2F, there was no decline of  $[Ca^{2+}]_i$  following removal of external  $Ca^{2+}$  in the presence of  $La^{3+}$  but, as soon as the trivalent cation had been removed,  $[Ca^{2+}]_i$  started to decrease. These experiments confirm that NCX has at most a very minor role in cytosolic  $Ca^{2+}$  clearance in pancreatic acinar cells.

#### Overexpression of Bcl-2 Slows Down $Ca^{2+}$ Extrusion in AR42J Cells

In order to test further the role of Bcl-2 in regulating  $Ca^{2+}$  extrusion, we stably overexpressed Bcl-2 in a pancreatic acinar cell line (AR42J) and then assessed the rate of recovering the basal  $[Ca^{2+}]_i$  after an imposed period of elevated  $[Ca^{2+}]_i$  using our

standard protocol (Figures 1A and 1B). In these experiments we measured  $[Ca^{2+}]_i$  using two independent methods: cytoplasmic calcium Cameleon YC3.60 (Figures 1G, S3A, and S3B) and Fura-2 (Figures S3C–S3E).  $Ca^{2+}$  extrusion in cells overexpressing Bcl-2 was substantially slower than in control cells in both these series of experiments (Figures 1G and S3E), confirming a role for Bcl-2 in regulation of  $Ca^{2+}$  extrusion. Bcl-2 must act by inhibiting PMCA because in these cells,  $Ca^{2+}$  extrusion was also independent of the presence or absence of external  $Na^+$  (Figures S3A–S3D). The increased level of Bcl-2 in the overexpressing cells was confirmed by western blot analysis (Figure 2D).

#### Bcl-2 Regulates $Ca^{2+}/Ba^{2+}$ Influx in Pancreatic Acinar Cells

In the presence of external  $Ca^{2+}$ , there will inevitably be both  $Ca^{2+}$  entry and  $Ca^{2+}$  extrusion, and it was therefore of interest also to test the possible effect of Bcl-2 on  $Ca^{2+}$  entry alone. Because  $Ba^{2+}$  is not extruded by the  $Ca^{2+}$  pump but does pass through  $Ca^{2+}$  channels, we used  $Ba^{2+}$  in the external solution rather than  $Ca^{2+}$  in these experiments [13]. Comparisons of the averaged  $Ba^{2+}$  entry traces (Figure 2A) and the half-times of the rises in the intracellular  $[Ba^{2+}]_i$  (Figure 2B) show that the rate of  $Ba^{2+}$  entry is significantly enhanced in Bcl-2 KO cells as compared to WT cells. However, the effect of Bcl-2 on  $Ca^{2+}/Ba^{2+}$  entry is quantitatively

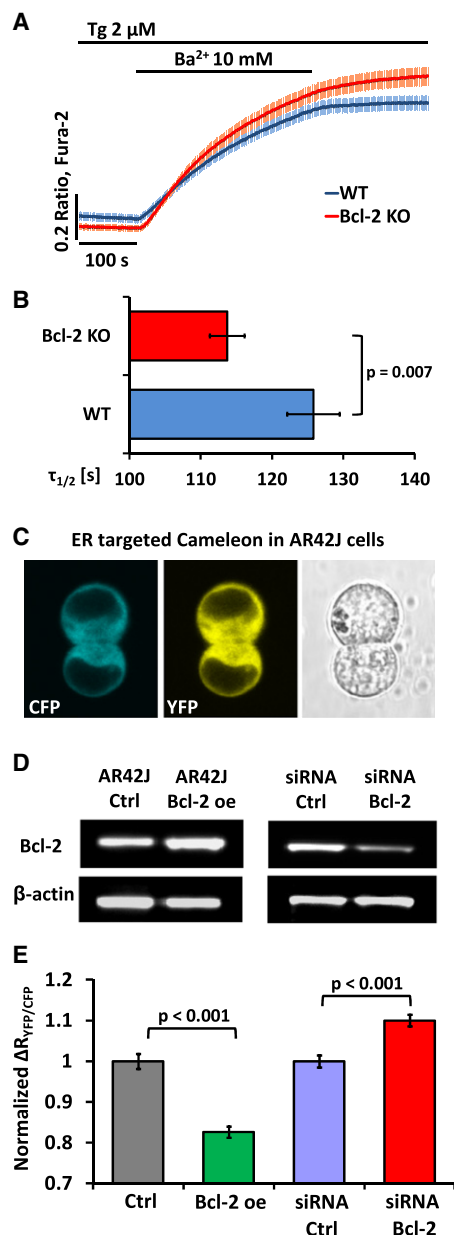


**Figure 2.** Effects of Bcl-2 on Ca<sup>2+</sup>/Ba<sup>2+</sup> Influx and [Ca<sup>2+</sup>]<sub>ER</sub>  
(A) Changes in the average [Ba<sup>2+</sup>], following introduction of an external solution containing 10 mM Ba<sup>2+</sup> in the continued presence of Tg, recorded in WT (blue trace, n = 60) and Bcl-2 KO (red trace, n = 61) pancreatic acinar cells. Traces are shown with standard errors. Data in (A), (B), and (E) are presented as mean  $\pm$  SEM.  
(B) Bar chart comparing half-times ( $\tau_{1/2}$ ) of the rise in Ba<sup>2+</sup>-induced Fura-2 ratio toward a plateau in WT (blue bar, n = 60) and Bcl-2 KO (red bar, n = 61) pancreatic acinar cells (shown in A).  
(C) An AR42J cell doublet transfected with D1ER Cameleon. Blue fluorescence comes from the CFP component and yellow fluorescence from YFP.  
(D) Results of immunoblotting against Bcl-2 performed on total protein isolated from (from left to right) control untransfected AR42J cells, AR42J cells stably transfected with pcDNA3 plasmid containing human Bcl-2 insert, AR42J cells transfected with control (scrambled) siRNA, and AR42J cells transfected with Bcl-2 siRNA.  $\beta$ -actin is shown as loading control. See also Figure S4 for distribution of Bcl-2 in pancreatic acinar cells and AR42J cells.  
(E) Bar chart comparing differences in resting [Ca<sup>2+</sup>]<sub>ER</sub>, presented as the difference between basal YFP/CFP values and YFP/CFP values obtained after treatment with 20  $\mu$ M CPA, normalized to controls. The gray bar

much smaller than the effect on Ca<sup>2+</sup> extrusion (Figures 1A, 1B, and 1E).

#### Bcl-2 Regulates the Resting Ca<sup>2+</sup> Levels in the ER

It was shown previously [3, 14] that Bcl-2 overexpression reduces Ca<sup>2+</sup> loading of the ER stores affecting Ca<sup>2+</sup> leak and uptake. This has been confirmed by some laboratories [15, 16], but not by others [17, 18]. We measured the resting [Ca<sup>2+</sup>]<sub>ER</sub> ([Ca<sup>2+</sup>]<sub>ER</sub>) of AR42J cells [19] with ER-targeted D1ER Cameleon (Figure 2C) [16, 20, 21] in untransfected AR42J cells, cells stably transfected with human Bcl-2, cells transiently transfected with Bcl-2-siRNA, and cells transiently transfected with control (scrambled) siRNA. The relative levels of Bcl-2 in control and Bcl-2-overexpressing AR42J cells are shown in Figure 2D. Cells from each group were treated with the SERCA inhibitor cyclopiazonic acid (CPA) in order to liberate the releasable Ca<sup>2+</sup> from the ER, and changes in the ratio YFP/CFP were compared. The results shown in Figure 2E demonstrate that Bcl-2 overexpression caused a decrease in resting [Ca<sup>2+</sup>]<sub>ER</sub> ( $0.83 \pm 0.013$  SE, n = 97, p < 0.001 as compared to  $1.00 \pm 0.018$  SE, n = 78 in untransfected control cells; arbitrary units), whereas the opposite effect was obtained by knocking down Bcl-2 with specific siRNA ( $1.10 \pm 0.014$  SE, n = 62, p < 0.001 as compared to  $1.00 \pm 0.015$  SE, n = 69 with scrambled siRNA; arbitrary units). Our data are in line with the majority of previous studies [3, 14–16] suggesting that the Ca<sup>2+</sup> leak channel in the ER [3, 15] and possibly the SERCA [22, 23] are regulated by Bcl-2. Our finding also underlines the necessity to assess [Ca<sup>2+</sup>]<sub>ER</sub> directly, because indirect cytosolic measurements can be misleading with regard to information about ER Ca<sup>2+</sup> loading.

#### Loss of Bcl-2 Protects against Necrosis and Promotes Apoptosis

In order to investigate the pathophysiological importance of Bcl-2 and in particular its regulation of Ca<sup>2+</sup> extrusion, we performed cell death assays on freshly isolated WT and Bcl-2 KO pancreatic acinar cells treated with 30  $\mu$ M menadione [24] and/or high external [Ca<sup>2+</sup>] (5 mM) for 30 min. Control groups were incubated for 30 min without any treatment. Our results (Figures 3A and 3B) show that untreated WT and Bcl-2 KO cells are characterized by very similar levels of apoptosis and necrosis. A high (5 mM) external [Ca<sup>2+</sup>] reduced the number of live WT cells in comparison to WT controls (p = 0.019). The same phenomenon was not observed in Bcl-2 KO cells (p = 0.05). Menadione (30  $\mu$ M) caused a substantial reduction in live WT cells in comparison to WT controls (p < 0.001), increasing both apoptosis (p < 0.001) and necrosis (p = 0.01). Treatment of WT cells with both menadione and high Ca<sup>2+</sup> increased necrosis even more than treatment with menadione alone (p = 0.018). Bcl-2 KO cells treated with 30  $\mu$ M menadione had decreased numbers of live cells (p = 0.001) and markedly increased numbers of apoptotic cells (p = 0.003) in comparison to the untreated Bcl-2 KO cells. However, necrosis levels were not significantly different when compared to the Bcl-2 KO control (p = 0.138). Combined treatment with menadione and 5 mM Ca<sup>2+</sup> did not substantially increase necrosis levels above those induced by menadione alone (p = 0.282). Importantly,

represents control, untransfected AR42J cells (n = 78), the green bar represents cells transfected with pcDNA3 plasmid containing human Bcl-2 insert (n = 97), the blue bar represents AR42J cells transfected with scrambled siRNA (n = 69), and the red bar represents AR42J cells transfected with Bcl-2 siRNA (n = 62).

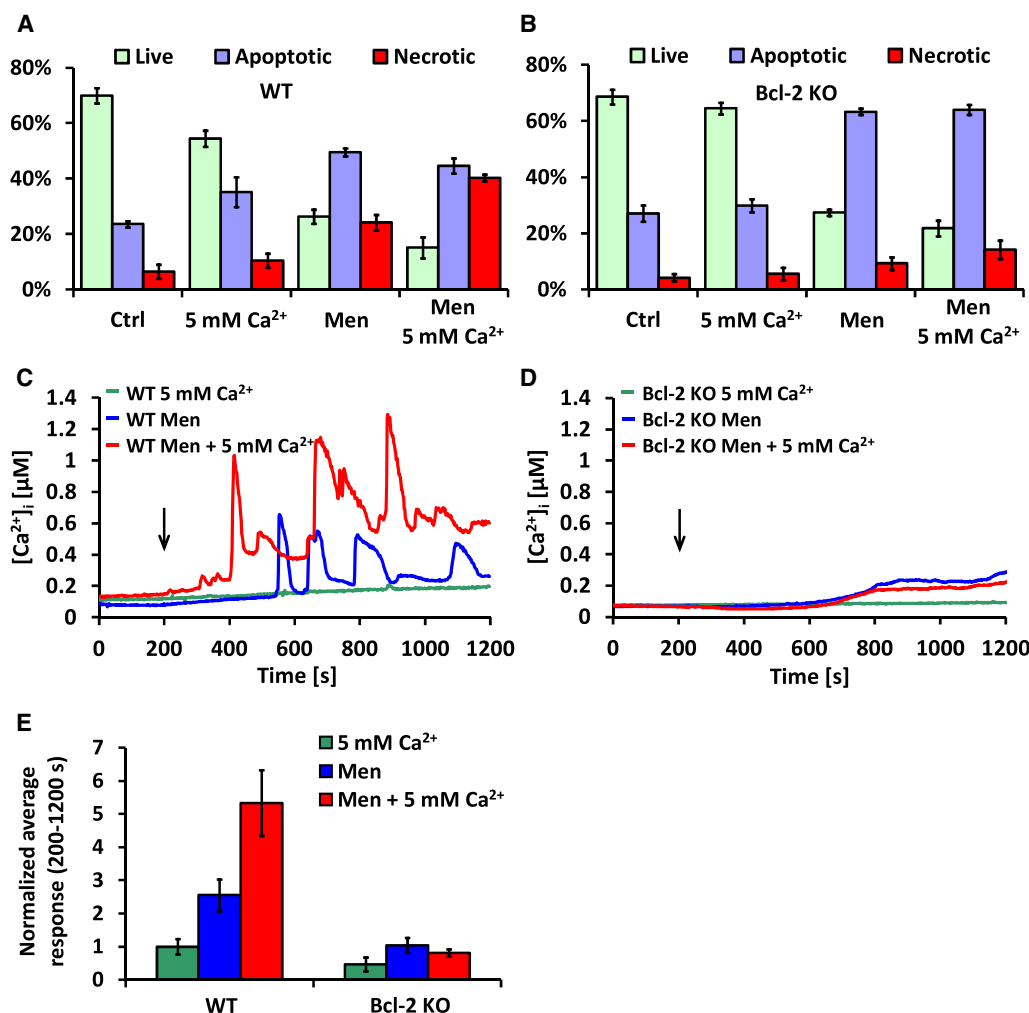


**Figure 3.** Bcl-2-Induced Inhibition of  $\text{Ca}^{2+}$  Extrusion Is Responsible for Higher Levels of Necrosis When Cells Are Stressed by Raised External  $[\text{Ca}^{2+}]$  and/or by Menadione

(A) Results of cell death assays performed on WT pancreatic acinar cells. Light green bars represent live cells, blue bars represent apoptotic cells, and red bars represent necrotic cells. The chart is separated into four treatment groups, from the left: untreated control cells, cells treated with 5 mM  $\text{Ca}^{2+}$ , cells treated with 30  $\mu\text{M}$  menadione, and cells treated with both 30  $\mu\text{M}$  menadione and 5 mM  $\text{Ca}^{2+}$ . Error bars in (A), (B), and (E) represent SEM.

(B) Results of cell death assays performed on Bcl-2 KO pancreatic acinar cells. The chart is structured in the same way as in (A), which allows comparison of the differences between WT and Bcl-2 KO cells. Cells lacking Bcl-2 undergo more apoptosis and less necrosis as compared to WT cells when challenged with 30  $\mu\text{M}$  menadione or both menadione and high  $\text{Ca}^{2+}$ .

(C) Typical  $[\text{Ca}^{2+}]_i$  responses to 5 mM  $\text{Ca}^{2+}$  (green,  $n_{\text{WT}} = 18$ ), 30  $\mu\text{M}$  menadione in 1 mM  $\text{Ca}^{2+}$  solution (blue,  $n_{\text{WT}} = 23$ ), and 30  $\mu\text{M}$  menadione in 5 mM  $\text{Ca}^{2+}$  (red,  $n_{\text{WT}} = 22$ ) in WT pancreatic acinar cells. Black arrow shows time point when treatment was applied.

(D) Typical  $[\text{Ca}^{2+}]_i$  responses to 5 mM  $\text{Ca}^{2+}$  (green,  $n_{\text{Bcl-2}} = 12$ ), 30  $\mu\text{M}$  menadione in 1 mM  $\text{Ca}^{2+}$  solution (blue,  $n_{\text{Bcl-2}} = 14$ ), and 30  $\mu\text{M}$  menadione in 5 mM  $\text{Ca}^{2+}$  (red,  $n_{\text{Bcl-2}} = 12$ ) in Bcl-2 KO pancreatic acinar cells. Black arrow shows time point when treatment was applied.

(E) The responses depicted in (C) and (D) were quantitatively analyzed and shown as the average  $[\text{Ca}^{2+}]_i$  responses above the baseline recorded between 200 and 1,200 s and then normalized to the average value of responses to 5 mM  $\text{Ca}^{2+}$  in WT cells. Green bars represent cells treated with 5 mM  $\text{Ca}^{2+}$ , blue bars represent cells treated with 30  $\mu\text{M}$  menadione, and red bars represent cells treated with both 30  $\mu\text{M}$  menadione and 5 mM  $\text{Ca}^{2+}$ . Responses of WT cells to menadione were greater than those recorded in Bcl-2 KO cells and were additionally potentiated by high extracellular  $\text{Ca}^{2+}$ .

Bcl-2 KO cells treated with menadione had increased apoptosis levels and decreased necrosis levels as compared to WT cells treated in the same way ( $p = 0.002$  and  $p = 0.016$ , respectively). Necrosis inhibition in Bcl-2 KO versus WT cells was even more pronounced between the groups incubated with menadione and high  $\text{Ca}^{2+}$  ( $p = 0.008$ ).

We also compared the rise in  $[\text{Ca}^{2+}]_i$  in Fura-2-loaded WT cells and Bcl-2 KO cells in response to menadione (30  $\mu\text{M}$ ) or to raising the external  $[\text{Ca}^{2+}]$  from 1 to 5 mM or to both raising  $[\text{Ca}^{2+}]_o$  to 5 mM and simultaneously adding menadione. Typical traces are shown in Figures 3C and 3D. An increase

in  $[\text{Ca}^{2+}]_o$  from 1 mM to 5 mM resulted in a small, slowly developing elevation of  $[\text{Ca}^{2+}]_i$  in WT cells but had almost no effect on Bcl-2 KO cells (green traces, Figures 3C and 3D). In both WT and Bcl-2 KO cells, treatment with menadione caused a slow elevation of  $[\text{Ca}^{2+}]_i$ . However, WT cells additionally responded with robust oscillations on top of the increasing  $[\text{Ca}^{2+}]_i$  baseline (blue trace, Figure 3C). These oscillations were markedly potentiated in the presence of 5 mM  $\text{Ca}^{2+}$  (red trace, Figure 3C). In contrast, cells lacking functional Bcl-2 protein did not develop such oscillations in response to menadione (blue trace, Figure 3D), and an increased  $[\text{Ca}^{2+}]_o$  had no further



effect on menadione-elicited responses in those cells (red trace, Figure 3D). Figure 3E summarizes the effects of menadione and high extracellular  $\text{Ca}^{2+}$  on WT and Bcl-2 KO cells. The responses are presented as averaged areas under the traces between 200 and 1,200 s calculated in the same way for each treatment and subsequently normalized to the average values of responses to 5 mM  $\text{Ca}^{2+}$  in WT cells. Responses to 5 mM  $\text{Ca}^{2+}$  appear to be lower in Bcl-2 KO cells as compared to WT cells, although the difference is not statistically significant ( $p = 0.105$ ). Menadione applied in the presence of both 1 mM and 5 mM extracellular  $\text{Ca}^{2+}$  induced much larger responses in WT cells as compared to Bcl-2 KO cells ( $p = 0.007$  and  $p < 0.001$ , respectively). In WT cells, the presence of 5 mM  $\text{Ca}^{2+}$  together with menadione caused much larger responses than menadione alone ( $p = 0.017$ ), whereas in Bcl-2 KO cells, the presence of 5 mM  $\text{Ca}^{2+}$  did not affect menadione-dependent responses ( $p = 0.38$ ). These data demonstrate that removal of Bcl-2 affords a remarkable degree of protection against attempts to raise  $[\text{Ca}^{2+}]_i$  by elevation of the external  $\text{Ca}^{2+}$  and/or stimulation with menadione.

#### Inhibition of PMCA by Caloxin 3A1 Promotes Necrosis

We studied the physiological importance of PMCA-mediated  $\text{Ca}^{2+}$  extrusion by using the specific PMCA inhibitor peptide caloxin 3A1 [25]. Figure 4A shows typical changes in  $[\text{Ca}^{2+}]_i$  in response to Tg and ACh in normal control pancreatic acinar cells as compared to cells preincubated for 300 s in the presence of caloxin 3A1. Caloxin 3A1 increased the basal resting  $[\text{Ca}^{2+}]_i$  and significantly inhibited  $\text{Ca}^{2+}$  extrusion (Figure 4A), effectively doubling the half-time of recovery of the prestimulation  $[\text{Ca}^{2+}]_i$  (Figure 4B). Caloxin 3A1 by itself did not increase the proportion of necrotic cells (Figure 4C) during relatively short (30 min) experiments, but it dramatically increased the proportion of necrotic cells when it was combined with menadione (Figure 4C).

#### Localization of Bcl-2

The mechanism by which Bcl-2 influences PMCA-mediated  $\text{Ca}^{2+}$  extrusion from pancreatic acinar cells needs to be explored in future studies. Localization studies (Figures S4A–S4C) indicate that Bcl-2 is widely expressed, in both pancreatic acinar cells and AR42J cells, including in the ER. Given that it is clear that the ER can come very close to the plasma membrane in pancreatic acinar cells [26], it is not surprising that PMCA and Bcl-2 are partly colocalized (Figures S4A–S4C). This clearly cannot be taken as evidence for a direct interaction between these two proteins but does not exclude such an interaction.

#### Conclusions

Our results reveal a new and unexpected role for Bcl-2 in the regulation of cellular  $\text{Ca}^{2+}$  homeostasis. In addition to the previously reported effects on  $\text{Ca}^{2+}$  signaling [3–5], we now show that Bcl-2 can suppress PMCA-mediated cellular  $\text{Ca}^{2+}$  extrusion and that such an inhibition has consequences for cell fate. Our data show that Bcl-2 KO cells are protected against the adverse effects of high extracellular  $\text{Ca}^{2+}$ , because they can extrude cytosolic  $\text{Ca}^{2+}$  more efficiently than WT cells. Furthermore, loss of Bcl-2 protein strongly promotes apoptosis and at the same time protects against excessive necrosis when cells are challenged with an agent (menadione) generating reactive oxygen species.

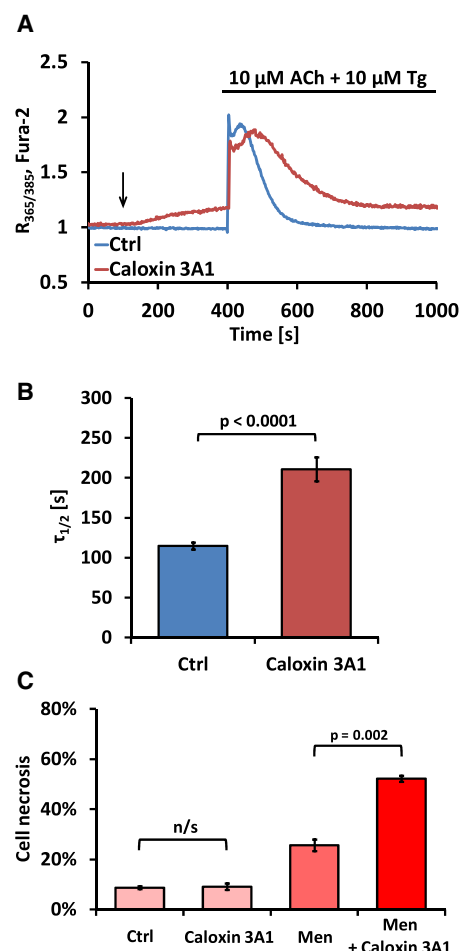


Figure 4. Specific Inhibition of PMCA Substantially Increases Necrosis in Pancreatic Acinar Cells

(A) Typical  $[\text{Ca}^{2+}]_i$  changes in response to 10  $\mu\text{M}$  Tg and 10  $\mu\text{M}$  acetylcholine (ACh) in an untreated pancreatic WT pancreatic acinar cell (blue trace) or a WT cell exposed to 1 mM caloxin 3A1 (dark red trace). Black arrow indicates time of caloxin 3A1 application. Note the gradual increase in  $[\text{Ca}^{2+}]_i$  after caloxin 3A1 application.

(B) Bar chart comparing half-times ( $\tau_{1/2}$ ) of the reduction in  $[\text{Ca}^{2+}]_i$  to the resting level after responses to 10  $\mu\text{M}$  Tg and 10  $\mu\text{M}$  ACh in the presence (dark red bar,  $n = 26$ ) or absence (blue bar,  $n = 15$ ) of 1 mM caloxin 3A1. Error bars in (B) and (C) represent SEM.

(C) Bar chart comparing necrosis levels in WT pancreatic acinar cells under different conditions. Cells were incubated for 30 min in the presence of 1 mM caloxin 3A1, 30  $\mu\text{M}$  menadione, or 1 mM caloxin 3A1 and 30  $\mu\text{M}$  menadione. Control cells were incubated for the same amount of time, but without any treatment.

#### Experimental Procedures

Reagents used included Fluo-4/Fura-2 (Invitrogen), Tg (Calbiochem), collagenase (Worthington), HEPES and PBS (Lonza), PromoFectin (PromoKine), Bcl-2 pEGFP-C1 (Addgene 17999) and pcDNA3-Bcl-2 (Addgene 8768), rabbit anti-Bcl-2 antibodies (Abcam/Cell Signaling), mouse anti- $\beta$ -actin antibody (Santa Cruz), Bcl-2 siRNA (sc-29215, Santa Cruz), and scrambled siRNA-A (sc-37007, Santa Cruz). Cell culture reagents were supplied by GIBCO, and all other chemicals were purchased from Sigma (UK). Pancreatic acinar cells were isolated from WT or Bcl-2 KO C57BL6/J mice as described previously [24]. Transgenic mice (B6;129S2-Bcl-2) were obtained from The Jackson Laboratory (stock number 002265). All procedures were approved by local ethical review and covered by UK Home Office licenses. AR42J cells (ECACC, 93100618) were maintained in RPMI 1640 medium (GIBCO) [27].  $\text{Ca}^{2+}$  measurements were performed with Fluo-4 or Fura-2

[19, 27], cytosolic YC3.60 Cameleon [20, 21], or D1ER Cameleon [16].  $[Ca^{2+}]_i$  was calculated (Fura-2) and recovery phases were fitted with an exponential decay function [28]. Immunoblotting and immunofluorescence were performed as described previously [5, 26].

# Supplemental Information

Supplemental Information includes four figures and can be found with this article online at [doi:10.1016/j.cub.2012.05.002](https://doi.org/10.1016/j.cub.2012.05.002).

# Acknowledgments

O.H.P. is a Medical Research Council Professor (G19/22/2). This work was supported by program grants G0700167 and MR/J002771/1 from the Medical Research Council (UK). P.E.F. was a Wellcome Trust-funded PhD student. D1ER Cameleon was a gift from Roger Tsien, and YC3.60 was a gift from Atsushi Miyawaki.

Received: December 7, 2011

Revised: April 2, 2012

Accepted: May 1, 2012

Published online: June 14, 2012

# References

- Martinou, J.C., and Youle, R.J. (2011). Mitochondria in apoptosis: Bcl-2 family members and mitochondrial dynamics. *Dev. Cell* 21, 92–101.
- Kelly, P.N., and Strasser, A. (2011). The role of Bcl-2 and its pro-survival relatives in tumorigenesis and cancer therapy. *Cell Death Differ.* 18, 1414–1424.
- Pinton, P., Ferrari, D., Magalhães, P., Schulze-Osthoff, K., Di Virgilio, F., Pozzan, T., and Rizzuto, R. (2000). Reduced loading of intracellular  $Ca^{2+}$  stores and downregulation of capacitative  $Ca^{2+}$  influx in Bcl-2-overexpressing cells. *J. Cell Biol.* 148, 857–862.
- Monaco, G., Decrock, E., Akl, H., Ponsaerts, R., Vervliet, T., Luyten, T., De Maeyer, M., Missiaen, L., Distelhorst, C.W., De Smedt, H., et al. (2012). Selective regulation of IP3-receptor-mediated  $Ca^{2+}$  signaling and apoptosis by the BH4 domain of Bcl-2 versus Bcl-Xl. *Cell Death Differ.* 19, 295–309.
- Gerasimenko, J., Ferdek, P., Fischer, L., Gukovskaya, A.S., and Pandolf, S.J. (2010). Inhibitors of Bcl-2 protein family deplete ER  $Ca^{2+}$  stores in pancreatic acinar cells. *Pflugers Arch.* 460, 891–900.
- Rong, Y.P., Aromolaran, A.S., Bultynck, G., Zhong, F., Li, X., McColl, K., Matsuyama, S., Herlitz, S., Roderick, H.L., Bootman, M.D., et al. (2008). Targeting Bcl-2-IP3 receptor interaction to reverse Bcl-2's inhibition of apoptotic calcium signals. *Mol. Cell* 31, 255–265.
- Brini, M., and Carafoli, E. (2009). Calcium pumps in health and disease. *Physiol. Rev.* 89, 1341–1378.
- Berberián, G., Podjarny, A., Di Polo, R., and Beaugé, L. (2012). Metabolic regulation of the squid nerve  $Na^+/Ca^{2+}$  exchanger: recent kinetic, biochemical and structural developments. *Prog. Biophys. Mol. Biol.* 108, 47–63.
- Petersen, O.H. (2003). Localization and regulation of  $Ca^{2+}$  entry and exit pathways in exocrine gland cells. *Cell Calcium* 33, 337–344.
- Porras, O.H., Ruminot, I., Loaiza, A., and Barros, L.F. (2008).  $Na^+$ - $Ca^{2+}$  cosignaling in the stimulation of the glucose transporter GLUT1 in cultured astrocytes. *Glia* 56, 59–68.
- Voronina, S.G., Gryshchenko, O.V., Gerasimenko, O.V., Green, A.K., Petersen, O.H., and Tepikin, A.V. (2005). Bile acids induce a cationic current, depolarizing pancreatic acinar cells and increasing the intracellular  $Na^+$  concentration. *J. Biol. Chem.* 280, 1764–1770.
- Shimizu, H., Borin, M.L., and Blaustein, M.P. (1997). Use of  $La^{3+}$  to distinguish activity of the plasmalemmal  $Ca^{2+}$  pump from  $Na^+/Ca^{2+}$  exchange in arterial myocytes. *Cell Calcium* 21, 31–41.
- Bakowski, D., and Parekh, A.B. (2007). Voltage-dependent  $Ba^{2+}$  permeation through store-operated CRAC channels: implications for channel selectivity. *Cell Calcium* 42, 333–339.
- Pinton, P., Giorgi, C., Siviero, R., Zecchini, E., and Rizzuto, R. (2008). Calcium and apoptosis: ER-mitochondria  $Ca^{2+}$  transfer in the control of apoptosis. *Oncogene* 27, 6407–6418.
- Foyouzi-Youssefi, R., Arnaudeau, S., Borner, C., Kelley, W.L., Tschopp, J., Lew, D.P., Demareux, N., and Krause, K.H. (2000). Bcl-2 decreases the free  $Ca^{2+}$  concentration within the endoplasmic reticulum. *Proc. Natl. Acad. Sci. USA* 97, 5723–5728.
- Palmer, A.E., Jin, C., Reed, J.C., and Tsien, R.Y. (2004). Bcl-2-mediated alterations in endoplasmic reticulum  $Ca^{2+}$  analyzed with an improved genetically encoded fluorescent sensor. *Proc. Natl. Acad. Sci. USA* 101, 17404–17409.
- He, H., Lam, M., McCormick, T.S., and Distelhorst, C.W. (1997). Maintenance of calcium homeostasis in the endoplasmic reticulum by Bcl-2. *J. Cell Biol.* 138, 1219–1228.
- Chen, R., Valencia, I., Zhong, F., McColl, K.S., Roderick, H.L., Bootman, M.D., Berridge, M.J., Conway, S.J., Holmes, A.B., Mignery, G.A., et al. (2004). Bcl-2 functionally interacts with inositol 1,4,5-trisphosphate receptors to regulate calcium release from the ER in response to inositol 1,4,5-trisphosphate. *J. Cell Biol.* 166, 193–203.
- Baumgartner, H.K., Gerasimenko, J.V., Thorne, C., Ferdek, P., Pozzan, T., Tepikin, A.V., Petersen, O.H., Sutton, R., Watson, A.J.M., and Gerasimenko, O.V. (2009). Calcium elevation in mitochondria is the main  $Ca^{2+}$  requirement for mitochondrial permeability transition pore (mPTP) opening. *J. Biol. Chem.* 284, 20796–20803.
- Nagai, T., Sawano, A., Park, E.S., and Miyawaki, A. (2001). Circularly permuted green fluorescent proteins engineered to sense  $Ca^{2+}$ . *Proc. Natl. Acad. Sci. USA* 98, 3197–3202.
- Shimozono, S., Fukano, T., Nagai, T., Kirino, Y., Mizuno, H., and Miyawaki, A. (2002). Confocal imaging of subcellular  $Ca^{2+}$  concentrations using a dual-excitation ratiometric indicator based on green fluorescent protein. *Sci. STKE* 125, pl4.
- Kuo, T.H., Kim, H.R., Zhu, L., Yu, Y., Lin, H.M., and Tsang, W. (1998). Modulation of endoplasmic reticulum calcium pump by Bcl-2. *Oncogene* 17, 1903–1910.
- Dremina, E.S., Sharov, V.S., and Schöneich, C. (2006). Displacement of SERCA from SR lipid caveolae-related domains by Bcl-2: a possible mechanism for SERCA inactivation. *Biochemistry* 45, 175–184.
- Gerasimenko, J.V., Gerasimenko, O.V., Palejwala, A., Tepikin, A.V., Petersen, O.H., and Watson, A.J.M. (2002). Menadione-induced apoptosis: roles of cytosolic  $Ca^{2+}$  elevations and the mitochondrial permeability transition pore. *J. Cell Sci.* 115, 485–497.
- Pande, J., Mallhi, K.K., and Grover, A.K. (2005). Role of third extracellular domain of plasma membrane  $Ca^{2+}$ - $Mg^{2+}$ -ATPase based on the novel inhibitor caloxin 3A1. *Cell Calcium* 37, 245–250.
- Lur, G., Haynes, L.P., Prior, I.A., Gerasimenko, O.V., Feske, S., Petersen, O.H., Burgoyne, R.D., and Tepikin, A.V. (2009). Ribosome-free terminals of rough ER allow formation of STIM1 puncta and segregation of STIM1 from IP(3) receptors. *Curr. Biol.* 19, 1648–1653.
- Baumgartner, H.K., Gerasimenko, J.V., Thorne, C., Ashurst, L.H., Barrow, S.L., Chvanov, M.A., Gillies, S., Criddle, D.N., Tepikin, A.V., Petersen, O.H., et al. (2007). Caspase-8-mediated apoptosis induced by oxidative stress is independent of the intrinsic pathway and dependent on cathepsins. *Am. J. Physiol. Gastrointest. Liver Physiol.* 293, G296–G307.
- Henke, W., Cetinsoy, C., Jung, K., and Loening, S. (1996). Non-hyperbolic calcium calibration curve of Fura-2: implications for the reliability of quantitative  $Ca^{2+}$  measurements. *Cell Calcium* 20, 287–292.